Hydrology Research

Hydrology Research Vol 53 No 10, 1271 doi: 10.2166/nh.2022.033

Response of the winter soil moisture of different vegetation types to rainfall events in karst slope land

Ershuang Yuan, Qiuwen Zhou*, Weihong Yan, Dawei Peng and Yalin Wang

School of Geography and Environmental Science, Guizhou Normal University, Guiyang, Guizhou 550025, China
*Corresponding author. E-mail: zouqiuwen@163.com

ABSTRACT

Understanding the response of soil moisture of different vegetation types to rainfall in karst regions in winter is significant for implementing various ecological restoration projects. However, at present, the related research is mainly focused on non-winter seasons, and only few research exist on winter seasons. Therefore, in this study, four types of vegetation – grassland, arable land, shrubland, and forestland – were selected as sample plots in the Guanling County of southwestern Guizhou, China. The magnitude, time, and speed responses of soil moisture of the vegetation types to rainfall were calculated using the time-series data of soil moisture of different vegetation types. The results showed that the response of soil moisture differed between different vegetation types in winter and non-winter seasons in karst areas. Among the four vegetation types, soil moisture response magnitude to rainfall in grassland and arable land had a similar distribution pattern along different soil depths, whereas in scrubland and forestland, it decreased gradually along the soil depth. In addition, compared with other vegetation types, for grassland soil moisture, the response magnitude, response duration, and response speed to rainfall are the largest, longest, and fastest, respectively. Our study used quantitative indices to illustrate the response of soil moisture to rainfall for different vegetation types under a humid climate in a mid-subtropical zone on sloped, pure limestone land. The results of this study provide a scientific basis for the implementation of ecological restoration projects in karst areas.

Key words: karst, rainfall, response, soil moisture, vegetation, winter

HIGHLIGHTS

- Grassland, arable land, shrubland, and forestland were studied in karst regions during winter.
- Grassland rainfall response magnitude, duration, and speed were largest, longest, and fastest, respectively.
- Soil moisture increment of arable land significantly changed.
- Water holding capacity of shrubland and forestland was relatively poor.
- Grassland and arable land had relatively small interception effects.

1. INTRODUCTION

Soil moisture, rainfall, and vegetation are interactive processes (Andrew *et al.* 2003; Daniele *et al.* 2008; Eunhyung & Sanghyun 2019). Soil moisture affects the distribution of vegetation types (Le *et al.* 2013; Zhao *et al.* 2019). Moreover, the vegetation type is considered the main factor controlling soil moisture (Chen *et al.* 2007). Among them, vegetation characteristics, such as bush layers, affect the redistribution of rainfall, thereby affecting the replenishment and change of soil moisture (Duan *et al.* 2016). Therefore, if the response of soil moisture to rainfall for different vegetation types can be clearly understood, it would help understand the interactions between soil moisture, vegetation, and precipitation and may have scientific significance for guiding the implementation of various ecological restoration projects (Hou *et al.* 2018).

In recent years, increasing attention has been paid to the response of soil moisture to rainfall for different vegetation types. The results of their studies showed that in different periods, the response of soil moisture of different vegetation types to rainfall is different. For example, Li *et al.* (2015) found that there are significant differences in the response patterns of soil moisture to rainfall in vegetable and forestland soils throughout the year. Also, Tian *et al.* (2019) found that in the vegetation growing season, the profile distribution patterns of soil moisture response of shrubs and bare land vegetation are similar,

while the profile distribution patterns of meadows, high-coverage grasslands, and medium-coverage grasslands are significantly different.

The above research results provide effective method references and valuable information for further research in non-karst areas; however, the research results may not be applicable to karst areas because the properties of bedrock and soil are also important factors that affect the dynamic changes of soil moisture (Zhao *et al.* 2020). Compared with other areas, in karst areas, the bedrock is mostly carbonate rock and karstification is strong, which makes the soil layer thin in such areas and leads to broken ground surfaces (Deng *et al.* 2020) and strong soil permeability. These characteristics may cause the magnitude, speed, and time of soil moisture response to rainfall to be different from those in other regions. Thus, the response of soil moisture to rainfall in karst regions differs from that in other regions.

Previous research has focused on the response of soil moisture to rainfall for different vegetation types in karst regions (Zhang *et al.* 2011; Fu *et al.* 2016; Yolanda *et al.* 2016; Yang *et al.* 2019). For example, Yang *et al.* (2021) found that under the same rainfall conditions, the response time of grassland soil moisture to rainfall is shorter than that of soil moisture of farmland and bare land and that the sensitivity of soil moisture in grassland is higher than that in farmland and bare land. Zhou *et al.* (2019) found that with the increase in rainfall, the increase in the soil water content in forestland and shrubland is greater than that in bare land and grassland. These studies have also explained the response of soil moisture of different vegetation types to rainfall in terms of response magnitude and response time. However, the current studies on the response of soil moisture to rainfall mainly focus on non-winter seasons (Chen *et al.* 2010; Guo *et al.* 2016), and there is not enough research conducted during the winter season. Also, the changes in soil moisture in winter still form an important part of hydrological processes and affect vegetation restoration and ecological reconstruction. On the one hand, because the climate in the research region is a humid mid-subtropical monsoon climate and the temperature in winter is not too cold, some vegetations continue to grow (Wang *et al.* 2020). However, vegetation growth inevitably requires a certain amount of moisture to support it. In winter, when rainfall is not abundant, soil moisture conditions still threaten vegetation growth, which makes it particularly important to understand the response of soil moisture to rainfall in winter (Zhang *et al.* 2012; Li *et al.* 2019; Ding *et al.* 2020). On the other hand, although winter precipitation is relatively low in humid karst areas (Xiao *et al.* 2021), soil moisture changes are still an important part of the hydrological process. Moisture stored in shallow soil layers in karst areas (Chen *et al.* 2021) becomes more important for moisture storage during winter drought conditions (Fu *et al.* 2016; Yang *et al.* 2019). Therefore, the response of soil moisture of different vegetation types to rainfall in winter is still an important topic that needs to be studied accurately.

Hence, to investigate the dynamic response of soil moisture of different vegetation types to rainfall in winter, the response magnitude, response time, and response rate of soil moisture of different vegetation types to rainfall in different soil layers were calculated and the dynamic response of soil moisture to rainfall was analyzed. Thus, the soil hydrological processes related to rainfall for different vegetation types in karst areas were revealed, and important reference values for the key management parameters of water resources were provided.

2. MATERIALS AND METHODS

2.1. Study area

The experimental site is located in Guanling County, southwest of Guizhou Province, China. The geographic coordinates are 105°43′E and 25°44′N, and the elevation is 367–1,831 m. It belongs to the Wumeng Mountains and has large undulations. The types of landforms in this territory are complex and diverse, the surface is broken, and limestone is widely distributed, which makes it a typical karst landform. The climate is humid mid-subtropical monsoon with an average annual temperature of 16.2 °C. The annual rainfall ranges between 1,205.1 and 1,656.8 mm and is concentrated between June and August, comprising ~52–55% of the annual rainfall, while the rainfall in winter accounts for ~3–5% of the annual rainfall. The main soil type in the area is Rendzic Leptosols. Natural vegetation here mainly consists of forests, shrubs, grass, and other vegetation. The forestland is mostly evergreen broad-leaved forest mixed with a small number of deciduous trees and cypress forests. Artificial vegetation mainly consists of corn, plantain, emperor bamboo grass, and sugar cane.

2.2. Design of the sample plots

To eliminate the influence of environmental factors, apart from vegetation type and related factors, the sample plots were all located on an ~25° slope with a northeasterly aspect at an elevation of ~700 m. Due to the shallow soil layer of karst slope land, the sample plots selected in this study had a large amount of gravel that reached the bedrock (~30 cm below the

surface), and the soil thickness significantly varied. Therefore, the depth of the soil profile moisture observation was set to 20 cm. The main vegetation in this area is artificially planted corn and plantain in addition to secondary grasslands, shrubs, and forestland that have been naturally restored after the conversion of farmland. Four land cover types – arable land, secondary grassland, secondary shrubland, and secondary forestland – were chosen, and monitoring plots were set up for them. The vegetation information and soil background of the sample plots are shown in Table 1, and Figure 1 shows an overview of the sample plots and the distribution of their monitoring points.

2.3. Observation data collection

For each vegetation type, five monitoring points with a size of 5 m × 5 m, an interval of ~20 m, and four sample plots were randomly selected (a total of 20 monitoring points). The HOBO H21_USB soil moisture monitoring system was used at each monitoring point, and the ECH2O-5 probe (The METER Group, Inc., USA) was horizontally inserted in the soil layers at different depths (0–5 cm, 5–10 cm, 10–15 cm, and 15–20 cm). Real-time monitoring of soil moisture changes during rainfall was performed, the data collection frequency was 10 min, and the monitoring time was from July 5, 2019 to January 6, 2020. Considering the actual start and end dates of winter in the study area, soil moisture data for this study were selected from November 5, 2019 to January 6, 2020.

The HOBO RG3_M automatic recording rainfall thermometer observation map was used for capturing the rainfall data. Concerning the monitoring points of each vegetation type, two monitoring points were selected to place this type of rainfall thermometer on the forest surface to observe the penetrating rainfall in the forest and the near-surface temperature under the vegetation. The data collection frequency and the observation period were synchronized with the soil moisture data.

2.4. Experimental methods

In each plot, soil samples were collected from four soil layers (5, 10, 15, and 20 cm) to determine the soil properties. A 100-cm^3 ring knife was used (bottom surface: 20 cm^2, height: 5 cm) to collect undisturbed soil from the four soil layers of each sample plot to determine the bulk density, total porosity, capillary porosity, noncapillary porosity, and saturated hydraulic conductivity of the soil. The sampling time was July 5–21, 2019. The organic matter content of the soil was determined using the potassium dichromate titration method. Moreover, the mechanical composition of the soil was measured using a laser particle size analyzer.

The soil bulk density, soil porosity, saturated hydraulic conductivity, soil particle size, and organic matter content are important factors that affect the dynamic changes in soil moisture. In this study, they were used as auxiliary factors to explain the dynamic changes in soil moisture for different vegetation types.

2.5. Data analysis

There was a total of 20 monitoring points for the 4 sample plots, out of which there were 5 monitoring points for each sample plot. Each monitoring point was divided into four soil layers for monitoring. A total of 80 soil moisture probes were used to obtain time-series soil moisture data through probe monitoring. The average soil moisture time series for each soil layer of each vegetation type at the five monitoring points were calculated as the soil moisture time series of the soil layer of the vegetation type. The average value of the measurement results of the 20 soil samples at the 5 monitoring points and the 4 soil layers of each vegetation type was calculated as the soil properties.

Table 1 | Overview of sample plots of various vegetation types

Vegetation type of plot	Vegetation coverage (%)	Vegetation height (m)	Soil type	Soil texture	Soil bulk density (g/cm)	Soil organic matter content (g/kg)
Arable land	40	2	Rendzic Leptosols	Silty loam	1.22	28.95
Grassland	70	0.7	Rendzic Leptosols	Silty loam	1.15	49.23
Shrubland	85	3.4	Rendzic Leptosols	Silty loam	1.11	68.15
Forestland	95	15	Rendzic Leptosols	Silty loam	1.04	70.90

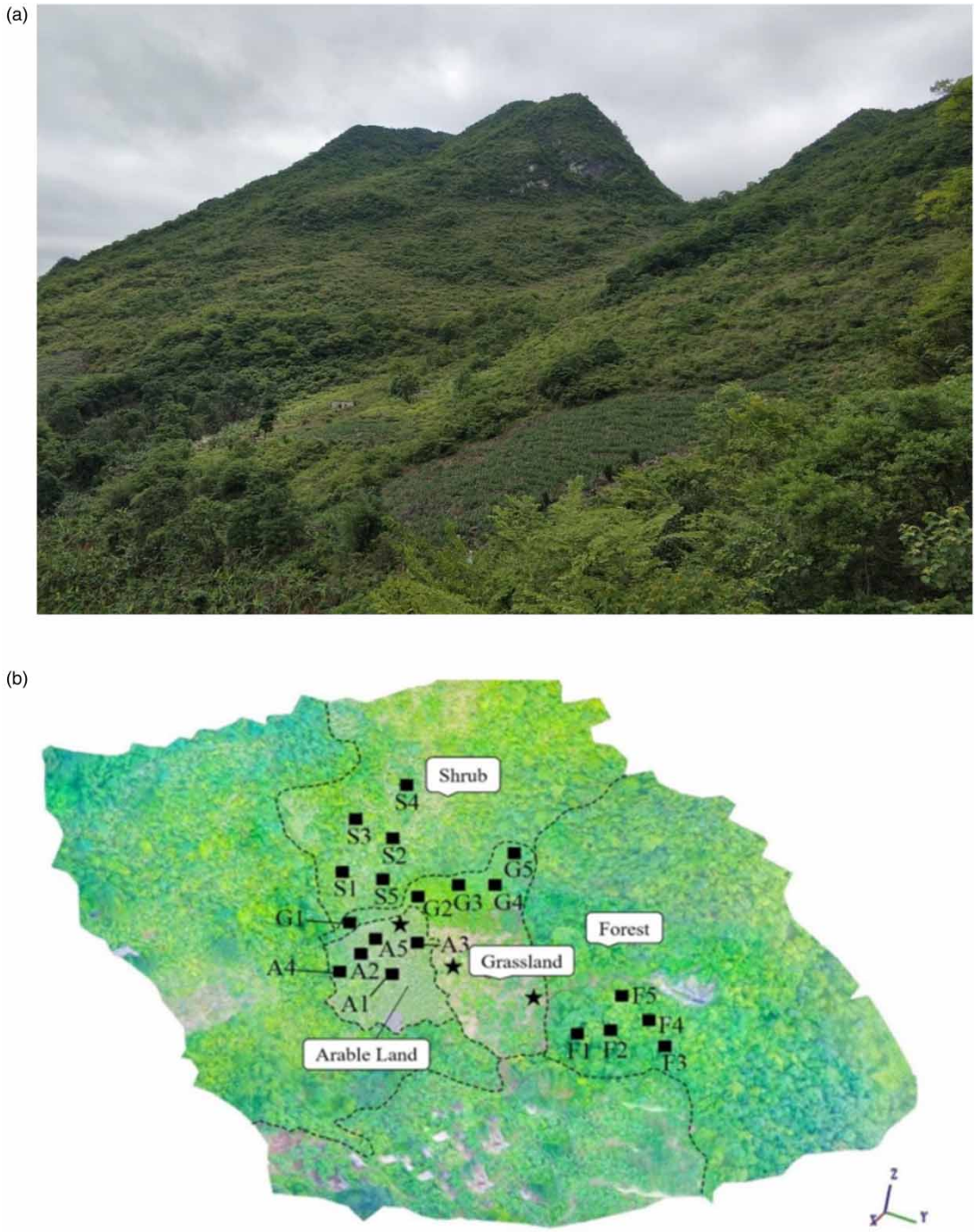

Figure 1 | (a) Overview map of the sample plots and (b) distribution map of the monitoring points. In (b), A1, A2, A3, A4, and A5 are arable land monitoring points; G1, G2, G3, G4, and G5 are grassland monitoring points; F1, F2, F3, F4, and F5 are forest land monitoring points; and S1, S2, S3, S4, and S5 are shrubland monitoring points. The dotted line separates the different vegetation from each other. ★ represents the automatic rainfall thermometer.

2.6. Identification of soil moisture in response to rainfall events

Usually, after rainfall, it can be assumed that the rainfall infiltration has reached a certain soil profile layer when its soil moisture starts to increase (Laio *et al.* 2001; Wang *et al.* 2008; Lozano-Parra *et al.* 2015). Therefore, the increase of soil moisture at

5, 10, 15, and 20 cm after rainfall was used to define and describe the soil response process. Hence, the rainfall impact period data was recorded 10 min before the beginning of rainfall to 12 h after the end of rainfall. Considering the accuracy of the soil moisture probe, a rainfall event with an increase in soil moisture of more than 0.2% (Lin & Zhou 2008) was considered an effective rainfall event. We then calculated the change in the soil moisture during rainfall. We used the time of the first soil moisture increase, which was greater than 0.2%, as the start of the soil response and the time of the soil moisture increase, which was less than 0.2%, as the end of the soil response.

There were 14 rainfall events during the observation period. According to the standards of the National Meteorological Administration of China, the rainfall events were then divided into light rain events and moderate rain events. Rainfall of less than 10 mm within 24 h was defined as light rainfall, and rainfall between 10 and 25 mm within 24 h was defined as moderate rainfall. Of the total rainfall events, 12 were light rainfall events and 2 were moderate rainfall events.

2.7. Quantification of soil moisture response

Quantification of soil moisture response can provide reference indicators for process-based soil hydrological modeling (Green & Erskine 2011; Clark *et al.* 2017). Therefore, in this study, we used a series of quantitative indicators to characterize the response of soil moisture to quantitatively describe the dynamic response of soil moisture to rainfall events under different vegetation types.

Several indicators have been used in previous studies to analyze the response magnitude of soil moisture to rainfall (Wiekenkamp *et al.* 2016; Mccoll *et al.* 2017). In this study, the absolute cumulative increase in soil moisture during a rainfall event was used as the response magnitude of the soil moisture to rainfall (ASWI). The formula is as follows:

$$\mathrm{ASWI}^j = \sum_{t=\mathrm{ST}}^{\mathrm{ET}} \Delta\theta^j_{t+} \tag{1}$$

$$\Delta\theta^j_{t+} \begin{cases} \Delta\theta^j_t, & \Delta\theta > 0 \\ 0, & \Delta\theta^j_t \le 0 \end{cases} \tag{2}$$

where θ^j_t is soil moisture at time t in the jth soil response event, Δt is the time interval (10 min), ST and ET denote the start and end time of the jth soil response event, respectively, and ASWI is the cumulative soil moisture increase of the soil response event. The ASWI of each soil layer at each monitoring point was calculated. To study the relationship between the increase in soil moisture in the upper and lower depths, we calculated the ratio of the increase in the soil moisture of two adjacent layers during the same rainfall event (RSWI):

$$\mathrm{RSWI}^j_i(\%) = 100 \times \mathrm{ASWI}^j_{i-1}/\mathrm{ASWI}^j_i \tag{3}$$

Among them, i represents the soil layer ($i = 2, 3, 4$) and ASWI^j_{i-1} and ASWI^I_i are the soil moisture increments of the $i-1$ and i layers in the jth soil response event, respectively.

This study is based on the time derivation of the increase in soil moisture, and the maximum slope and average slope of the soil response event were used to characterize the soil response rate. Among them, $S_{\max}$ and S_{mean} are the maximum and average rates of the soil response to events, respectively, in vol.%/min.

$$S_{\mathrm{mean}} = \mathrm{mean}\left(100 \times \frac{\theta_{t+\Delta t} - \theta_t}{\Delta t}\right) \tag{4}$$

$$S_{\max} = \max\left(100 \times \frac{\theta_{t+\Delta t} - \theta_t}{\Delta_t}\right) \tag{5}$$

According to Sun *et al.* (2015), the response time of soil moisture to rainfall can be divided into two periods: soil moisture response time (soil moisture begins to increase after rainfall) and the increase period of soil moisture (duration of the soil response event). The soil moisture response time difference between adjacent soil layers is used to describe the migration

process of the soil response peak and can be calculated using the following equation:

$$DRT_i = ST_i - ST_{i-1} \tag{6}$$

ST_{i-1} and ST_i are the response times ($i = 2, 3, 4$) of soil moisture in the $i-1$th and ith layers to rainfall events, respectively, and DRT is the response time difference. The soil response event duration is calculated according to the following equation:

$$Duration_j = ET_j - ST_j \tag{7}$$

Among them, ET_j and ST_j are the start and stop times of the jth soil response event, respectively.

3. RESULTS

3.1. Dynamic changes in soil moisture and rainfall during the monitoring period

As shown in Figure 2, the dynamic changes of soil moisture of different vegetation types according to the rainfall changes during the monitoring period and the variation of soil moisture in each soil layer are different. With the increase in rainfall, the soil moisture of various vegetation types significantly fluctuated. Among them, the grassland soil moisture significantly

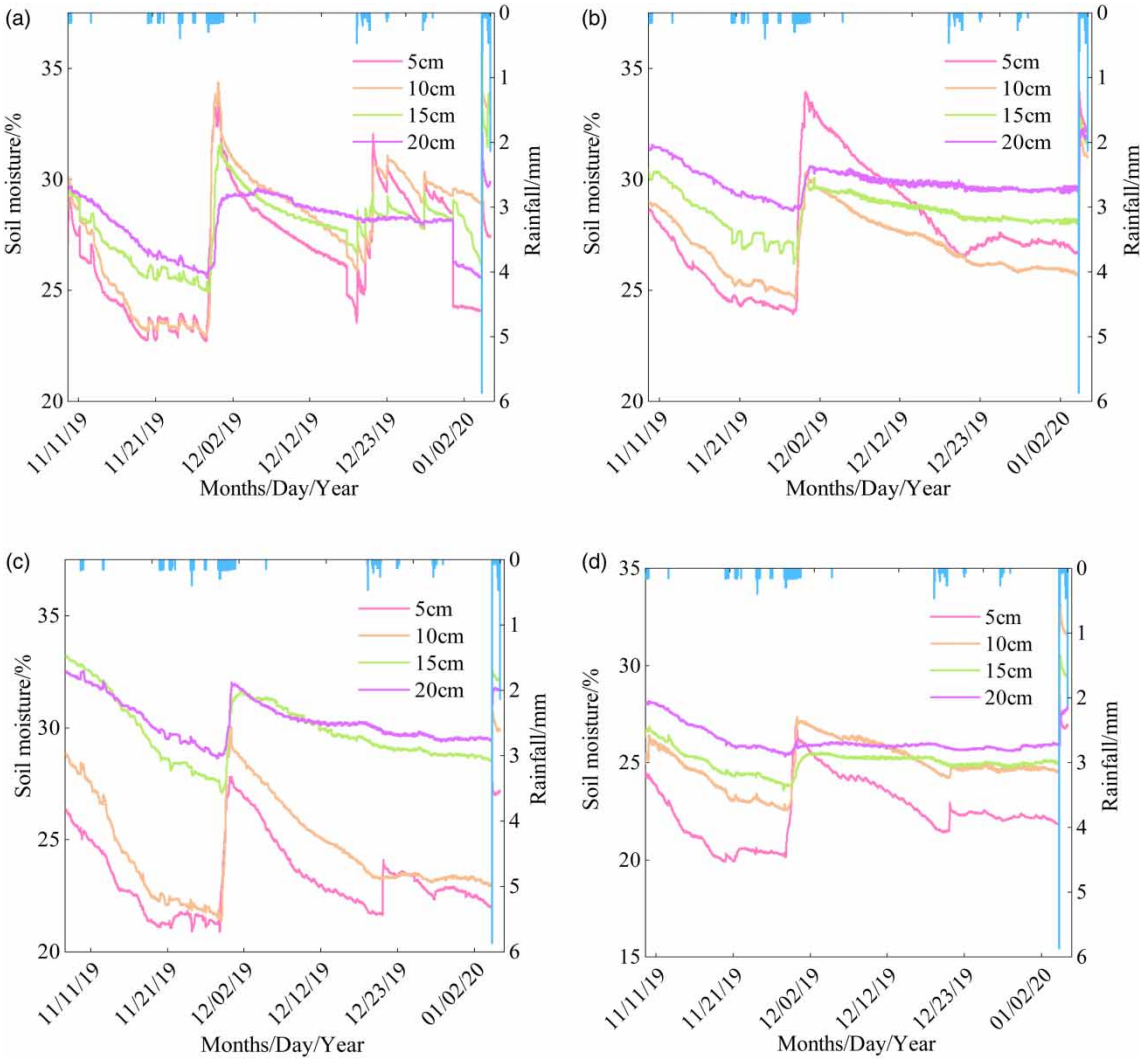

Figure 2 | Distribution diagram of soil moisture and rainfall time series of different vegetation types during the monitoring period. (a) Grassland, (b) arable land, (c) shrubland, and (d) forestland.

fluctuated with the change in rainfall (Figure 2(b)), and soil moisture of the shrub in different soil depths had obvious differences (Figure 2(c)).

3.2. Response magnitude of soil moisture for different vegetation types to different rainfall events

During light rainfall events, the magnitudes of the grassland and farmland soil moisture responses decreased with the increase in the soil layer (Figure 3). During moderate rainfall events, the maximum magnitude soil moisture responses of the grassland and arable land occurred in the second soil layer, and the maximum magnitude soil moisture responses of the shrubland and forestland occurred in the first soil layer.

By comparing the ASWI and RSWI of the different rainfall events (Figures 3 and 4), the response magnitudes of the grassland and shrubland soil moistures to moderate rainfall events were greater than that for light rainfall events. Compared with other vegetation types, grassland had the highest ASWI value, indicating that grassland soil moisture had the largest response to rainfall. The RSWI value for each layer of the arable land varied significantly.

3.3. Response time of soil moisture of different vegetation types to different rainfall events

As shown in Figure 5(a), during a light rainfall event, the difference in soil moisture response time (*DRT*) between adjacent grassland soil layers increased with the increase in the soil layer, and the maximum *DRT* value was observed in the third grassland layer. As shown in Figure 6(a), during a moderate rainfall event, the *DRT* of the different vegetation types increased in the following order: forestland < shrubland < grassland < arable land.

As shown in Figure 5(b), during a light rainfall event, the soil moisture response duration (*Duration*) of the grassland and arable land changed slightly within the same soil layer, and the maximum *Duration* was observed in the third grassland layer. As shown in Figure 6(b), during a moderate rainfall event, the *Duration* of each vegetation type varied significantly between the different soil layers, from 0.23 to 54 h. Compared with the other vegetation types, the *Duration* of each grassland soil layer was the highest, and the *Duration* in the case of moderate rainfall events was significantly greater than that in the case of light rainfall events.

This indicated that in the case of light rainfall, the grassland soil moisture response lasted longer than that of the arable land. Compared with the other vegetation types, in the case of moderate rainfall, the grassland soil moisture response was the longest, and the soil moisture response time difference between the adjacent soil layers of the shrubland was minimum.

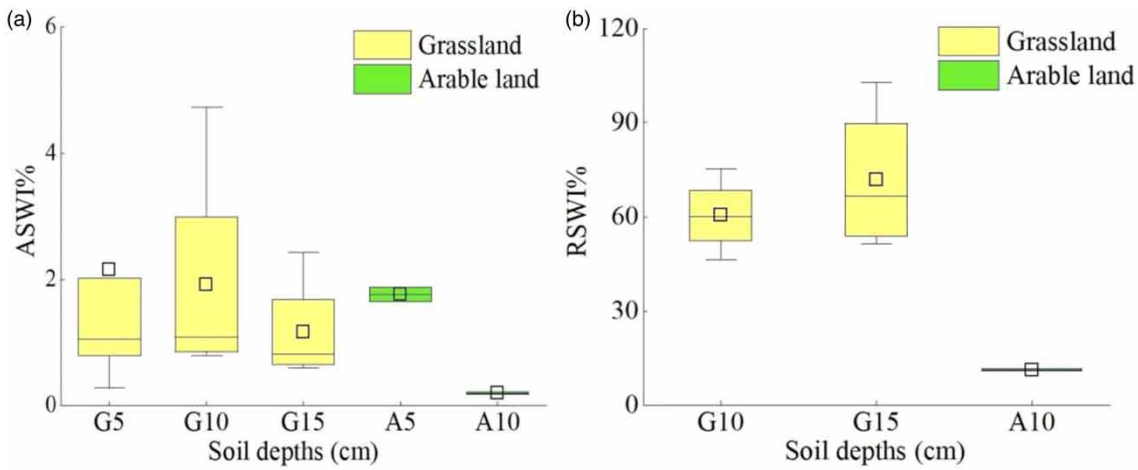

Figure 3 | (a) ASWI and (b) RSWI distribution diagrams of different vegetation types under light rainfall events. In the box diagram, G represents grassland and A represents arable land. ASWI, absolute cumulative increase in soil moisture; RSWI, ratio of the increase in soil moisture of the two adjacent depths. Note that only grassland and arable land soil moisture under small rain conditions respond, where the grassland response depth is 0–15 cm and the arable land response depth is 0–10 cm.

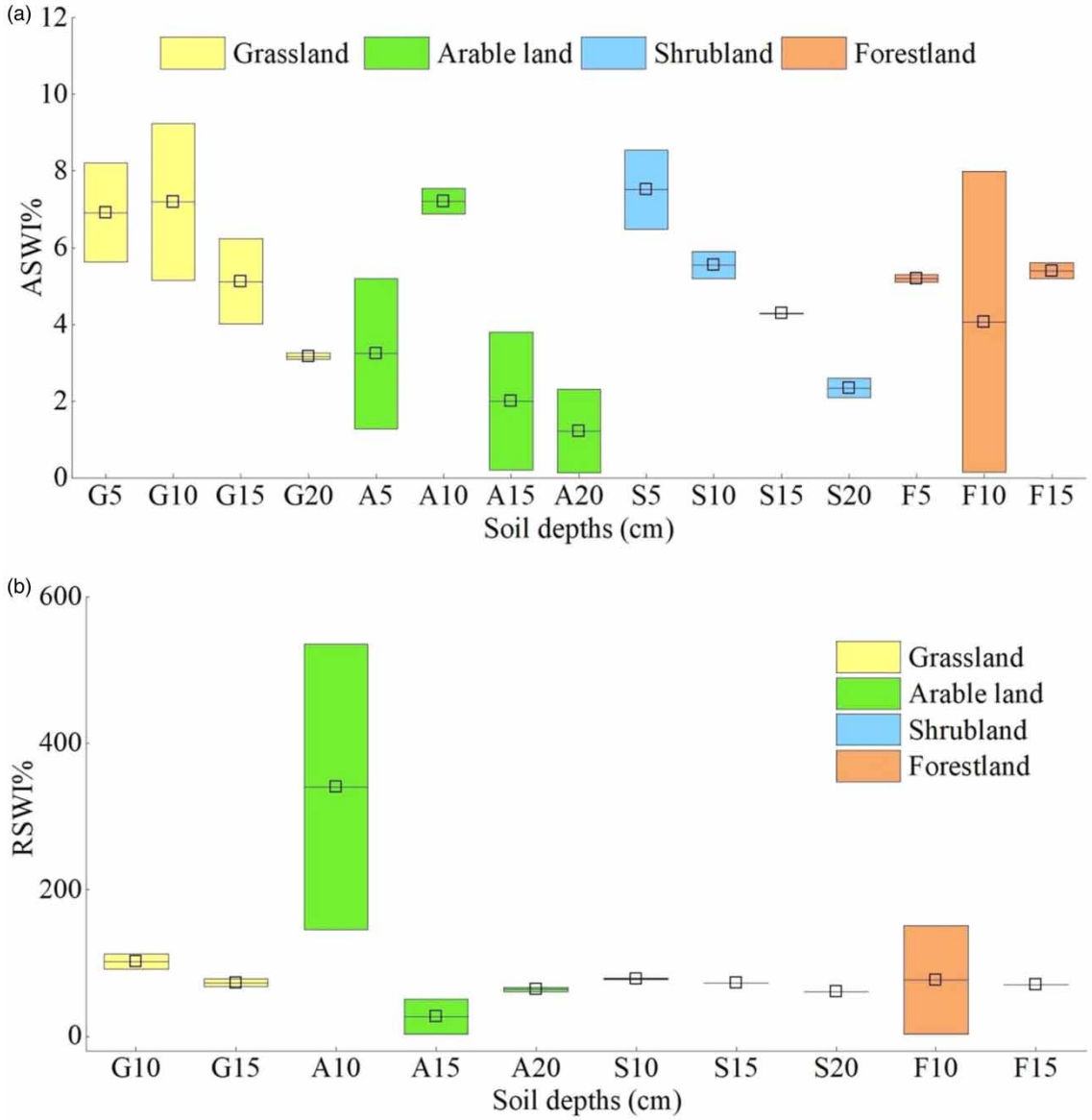

Figure 4 | ASWI (a) and RSWI (b) distribution map of different vegetation types under moderate rain events. G, (a), (s), and F stand for grassland, arable land, S shrubland, and forestland, respectively. Note that the soil moisture response depth of forest land is 0–15 cm.

3.4. Response speed of soil moisture of different vegetation types to different rainfall events

It can be seen from Figures 7 and 8 that in the case of light rain, the S_{max} and S_{mean} of the grassland and arable land decreased with the increase in the soil layer, and the response speed of the grassland was significantly higher than that of the arable land, where the response speed was fastest in the first layer. This shows that the response speed of soil moisture of various vegetation types under light rain events decreases with the increase in the soil layer. In the case of moderate rain, the response speeds of the soil moistures of different vegetation types were different; however, the highest values of S_{max} and S_{mean} appeared in the first grassland layer.

As shown in Figure 7, in the case of light rain, the S_{max} and S_{mean} of the grassland and arable land decreased with the increase in the soil layer, and S_{max} was the highest (1.62 vol.%/min) in the first layer. As shown in Figure 8, in the case of moderate rain, the S_{max} and S_{mean} of the first grassland layer and the farmland soil moisture were much higher than those of the other soil layers, indicating that the soil moisture response speed was fastest in this layer. In the case of moderate rain, the S_{max} and S_{mean} of the shrubs decreased with the increase in the soil layer. The S_{max} of the forestland increased

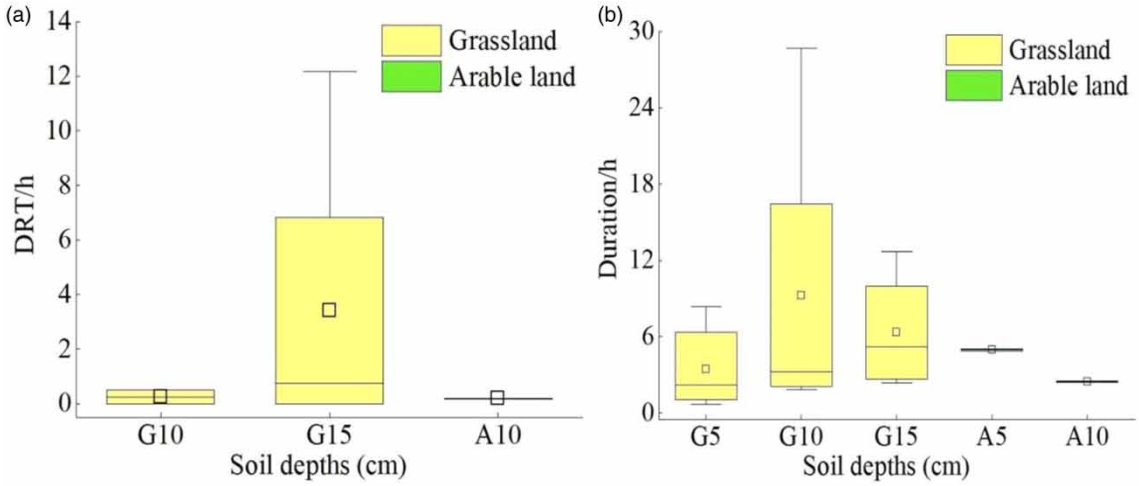

Figure 5 | *DRT* (a) and *Duration* (b) distribution maps of different vegetation types under light rain events. G represents grassland and A represents arable land. *DRT*: soil moisture response time difference between adjacent soil layers; *Duration*: soil response event duration.

and the S_{mean} decreased with the increase in the soil layer. In general, the response speed of soil moisture of all vegetation types was fastest in the first layer. The response speed of the soil moisture in the case of moderate rain was significantly greater than that of light rain, and the response speed of the grassland soil moisture to rainfall was significantly greater than those of the other vegetation types.

4. DISCUSSION

4.1. Response of the winter soil moisture of different vegetation types in karst areas

Through this study, it was found that compared with other vegetation types, karst slopes in grassland have the largest response to rainfall, longest response duration, and fastest response speed in winter. These results differ from the non-winter research results of Yang *et al.* (2021) in karst areas. Thus, the responses of soil moisture to rainfall for different vegetation types in karst areas in winter and non-winter seasons are different. The reason may be the seasonal difference in different vegetation types (Duan *et al.* 2016). For example, compared with forestland and shrubland, grassland in winter has less litter and low vegetation coverage. Compared with winter grassland, arable land has relatively high vegetation coverage and relatively large rainfall interception due to its dry winter crops. Therefore, compared with other vegetation types, the indicators of the grassland soil moisture response to rainfall in winter are larger than those of other vegetation types. In addition, in winter karst environments, compared with other vegetation types, the grassland vegetation coverage is low and the interception is relatively small. In addition, karst rock fissures are currently being developed (Li *et al.* 2020). After rainfall, most of the surface runoff quickly enters the ground along with rock fissures, resulting in faster and longer responses to rainfall in winter grassland.

Figure 3 shows that only the soil moisture of the arable land and grassland responded in the case of light rain. This may be due to the differences in the physical properties of soil (Peng *et al.* 2020). First, the saturated hydraulic conductivity, noncapillary porosity, and organic matter content of the shrubland and forestland were greater than those of the arable land and grassland (Figure 8), indicating that the water holding capacity of shrubland and forestland is relatively poor. In addition, in the karst areas, the soil layer was thin, and the bedrock had strong permeability (Chen *et al.* 2009), leading to the infiltration of most of the water in the shrubland and forestland when rainfall occurred. Second, compared with the shrubland and forestland, the grassland and arable land in the winter had relatively small interception effects, leading to light rain events, and soil moisture of the grassland and arable land could also respond. Figure 4 shows that the RSWI in the second layer (222.50%) of the arable land was greater than 100%, indicating that the cumulative increase in soil moisture of the arable land was maximum in the second layer. This may be because the saturated hydraulic conductivity of the arable land was the highest in the first layer and then gradually decreased with the increase in the soil layer (Figure 9). When rainfall occurred, the first soil moisture layer quickly infiltrated the second layer, making the under the same rainfall event. The cumulative increase in soil moisture of the arable land was maximum in the second layer.

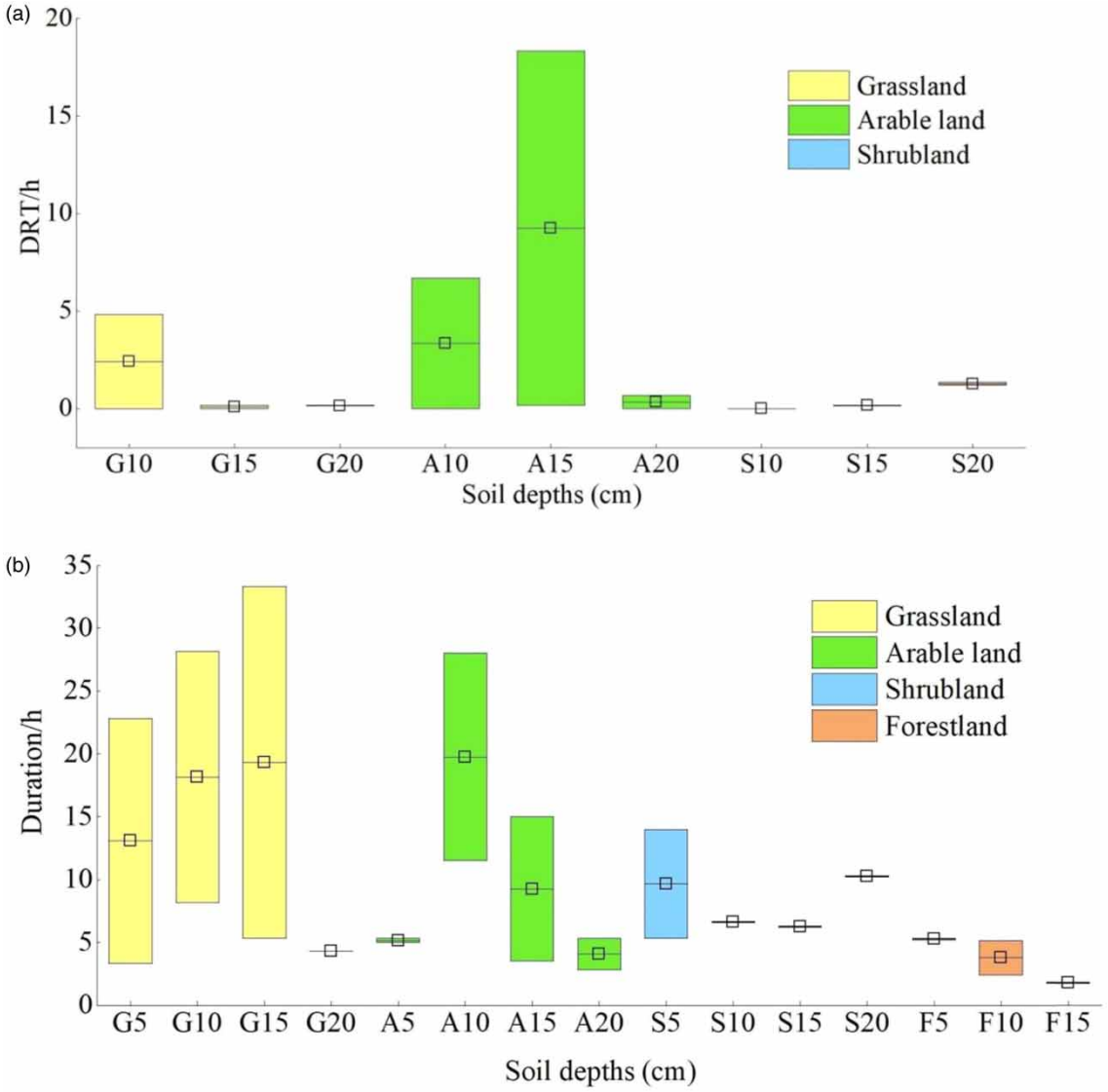

Figure 6 | *DRT* (a) and *Duration* (b) distribution maps of different vegetation types under moderate rain events. G, A, S, and F stand for grassland, arable land, shrubland, and forestland, respectively.

4.2. Impact of the karst environment on the research results

The geological background of karst areas is complex. Even if they are all carbonate rocks, the parent rock formed by the soil is different, and the soil bulk density, soil pore water, capillary water holding capacity, and other soil properties are different (Sheng *et al.* 2018). For example, the Rendzic Leptosols formed by calcareous dolomite were compared with the Rendzic Leptosols formed by pure limestone, which has strong water permeability, small water holding capacity, and low natural water content (Huang 1988). These differences in soil properties lead to differences in the response of soil moisture of different vegetation types during rainfall. The sample plots used in this study are located on a pure limestone slope, which only represents the response of the soil moisture of different vegetation types to rainfall on a pure limestone slope.

Second, karst areas have great spatial heterogeneity. Even if the bedrock is the same, the vegetation and seasonal characteristics of different climate types are different, which may cause differences in the response of soil moisture to rainfall (Chen *et al.* 2009). For example, in the same limestone karst area, in the case of a humid mid-subtropical climate, the seasonal vegetation differences are more obvious. In summer, the vegetation is dark green, and the canopy closure is relatively large. In autumn, yellowish-brown patches appear, and in winter, most leaves fall off, leaving only dry branches. In the semi-humid

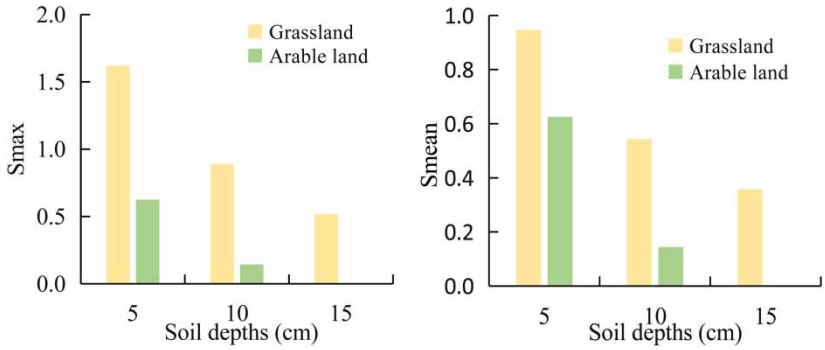

Figure 7 | Soil response rates of different vegetation types under light rain events (S_{max} and S_{mean}).

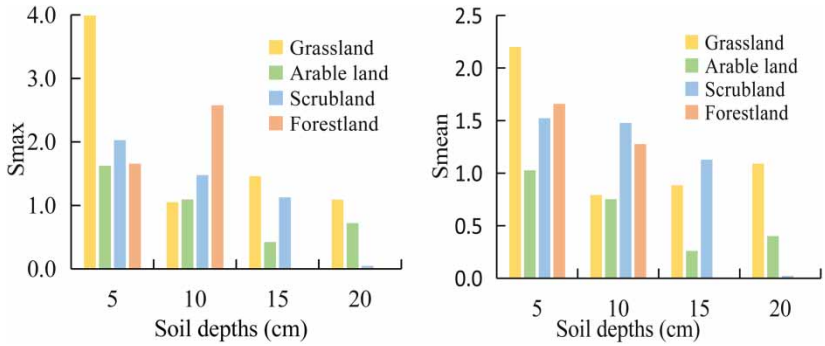

Figure 8 | Soil response rates of different vegetation types under moderate rain events (S_{max} and S_{mean}).

climate of South Asia, although vegetation significantly differs from summer to winter, only some dominant species are deciduous in winter and the forest layer is complex, where there are abundant plants in the middle forest layers, and the winding density of rattan (Huang 1988). These different vegetation characteristics may cause the interception of winter vegetation of this climate type to be greater than that of the mid-subtropical humid climate type, which may lead to differences in the response of winter vegetation soil moisture to rainfall (Chen *et al.* 2010). This study area belongs to the humid mid-subtropical climate, which only represents the response of different vegetation soil moistures to rainfall in this climate type, while the response of vegetation soil moisture to rainfall in other climate types needs further investigation.

In conclusion, this study can better explain the response of soil moisture to rainfall in winter for different vegetation types in the humid mid-subtropical monsoon climate of pure limestone slope land. The results of this study have enriched the understanding of the response of soil moisture of different vegetation types to rainfall in karst slopes and supplemented this knowledge system. This study also showed certain reference values for better understanding the interaction between the soil moisture, vegetation, and precipitation.

4.3. Limitations of the study

A limitation of this study is that it did not conduct enough replicate experiments, because our study area was not very large; therefore, we were unable to include several replicas of the sample plots. Additionally, to minimize the uncertainty caused by variations in lithology, soil, and climate, we wanted to ensure that the sample plots for all four vegetation types were located on a single slope. However, such locations were difficult to find. Even if a plot had been established in the vicinity of the study area, the topography or vegetation type could have varied, and topographic variation is another factor that affects soil water content (Gao *et al.* 2020). If the same plots had been established away from the study area, the climate, lithology, and soil conditions could have changed. This is particularly important in mountainous environments where there can be significant differences in local climates. In addition, the vegetation type at a sample site can change over years of monitoring. The study area has a humid subtropical monsoon climate with rapid vegetation growth that results in abandoned grassland usually being

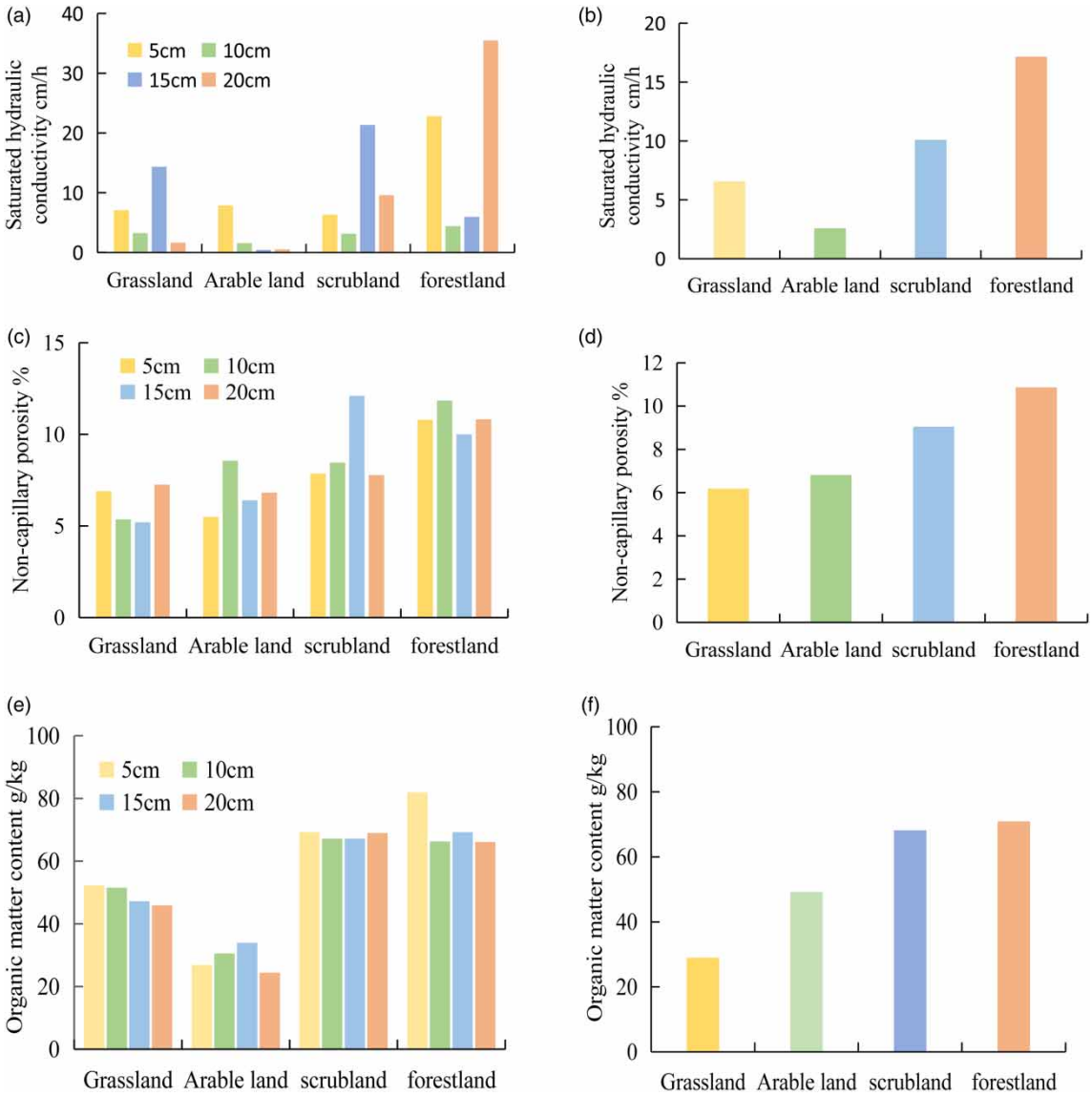

Figure 9 | Soil properties of different vegetation types. (a) Average profile saturated hydraulic conductivity, (b) saturated hydraulic conductivity, (c) average profile noncapillary porosity, (d) non-capillary porosity, (e) average profile organic matter content, and (f) organic matter content.

replaced by shrubs within a few years. For these reasons, it was difficult to prepare sufficient replication within the study. Therefore, the study did not use data from multiple winters.

4.4. Possible values

To improve the ecological environment in the karst region, since the 1990s, China has approved and implemented a large number of ecological restoration projects, for example, the Grain for Green Program and the Rocky Desertification Control Project (Li *et al.* 2022). Most ecological restoration projects not only aim to recover ecosystem structures and functions but also focus on improving human wellbeing (Qiu *et al.* 2022). Our results have two implications for vegetation restoration projects in karst regions. The first is that in humid karst areas, where vegetation can still grow during winter, winter soil moisture is an important part of the hydrological process. Therefore, the relationship between winter soil moisture and vegetation growth should not be ignored in the implementation of ecological restoration projects. The second is that in humid karst areas, the response pattern of soil moisture to rainfall is different for different vegetation types during the winter and non-

winter seasons. Therefore, when implementing ecological restoration projects, different ecological restoration modes should be selected according to local conditions and more attention should be paid to soil moisture storage in grasslands during winter.

5. CONCLUSION

In this study, to explain the response of soil moisture of four vegetation types to rainfall in karst areas in winter, the response magnitude, response time, and response speed of the soil moisture of different vegetation types to rainfall were calculated using the time-series data of soil moisture of different vegetation types.

The results showed that the response of soil moisture differed between different vegetation types in winter and non-winter seasons in karst areas. Among the four vegetation types, soil moisture response magnitude to rainfall in grassland and arable land had a similar distribution pattern along different soil depths, while in scrubland and forestland, it decreased gradually along the soil depth. In addition, compared with other vegetation types, for grassland soil moisture, the response magnitude, response duration, and response speed to rainfall were the largest, longest, and fastest, respectively. Overall, the findings of this study complement the understanding of the soil moisture of different vegetation types in karst slope land with regard to the rainfall response and enrich the related knowledge system. However, whether the response of soil water to rainfall in winter under other conditions, such as different bedrocks, climate types, vegetation types, and karst areas, will have new characteristics is a further question that needs further investigation.

AUTHORS' CONTRIBUTION

E.Y. and Q.Z. conceived and wrote the manuscript; W.Y. and D.P. were involved in the experimental assays; and Y.W. polished the language of the manuscript.

FUNDING

This work was supported by the Joint Fund of the National Natural Science Foundation of China and the Karst Science Research Center of Guizhou province [grant number U1812401]; the National Science Foundation of China [grant number 41761003]; the Scientific and Technological Research Project of Guizhou Province [grant number Qiankehe Jichu [2019]1433 and Qiankehe Pingtai Rencai [2017]5726]; and the Foundation Programme for Outstanding Talents in Higher Education Institutions of Guizhou Province [grant number [2018]042].

DATA AVAILABILITY STATEMENT

All relevant data are included in the paper or its Supplementary Information.

CONFLICT OF INTEREST

The authors declare there is no conflict.

REFERENCES

Andrew, W. W., Sen-Lin, Z., Rodger, B. G., Thomas, A. M., Günter, B. & David, J. W. 2003 Spatial correlation of soil moisture in small catchments and its relationship to dominant spatial hydrological processes. *Journal of Hydrology* **286** (1), 113–134.

Chen, H. S., Shao, M. G. & Li, Y. Y. 2007 Soil desiccation in the Loess Plateau of China. *Geoderma* **143** (1–2), 91–100.

Chen, X., Zhang, Z. C., Chen, X. H. & Shi, P. 2009 The impact of land use and land cover changes on soil moisture and hydraulic conductivity along the karst hillslopes of southwest China. *Environmental Earth Sciences* **59** (4), 811–820.

Chen, H. S., Zhang, W., Wang, K. L. & Fu, W. 2010 Soil moisture dynamics under different land uses on karst hillslope in northwest Guangxi, China. *Environmental Earth Sciences* **61** (6), 1105–1111.

Chen, F., Wang, S. J., Bai, X. Y., Liu, F., Zhou, D. Q., Tian, Y. C., Luo, G. G., Li, Q., Wu, L. H., Zheng, C., Xiao, J. Y., Qian, Q. H., Cao, Y., Li, H. W., Wang, M. M. & Yang, Y. Y. 2021 Assessing spatial-temporal evolution processes and driving forces of karst rocky desertification. *Geocarto International* **36** (3), 1–22.

Clark, M. P., Bierkens, M. F. P., Samaniego, L., Woods, R. A., Uijlenhoet, R., Bennett, K. E., Pauwels Valentijn, R. N., Cai, X. T., Wood Andrew, W. & Peters-Lidard, C. D. 2017 The evolution of process-based hydrologic models: historical challenges and the collective quest for physical realism. *Hydrology and Earth System Sciences* **21** (7), 3427–3440.

Daniele, P., Marco, B., Daniele, N. & Giancarlo, D. F. 2008 Hillslope scale soil moisture variability in a steep alpine terrain. *Journal of Hydrology* **364** (3), 311–327.

Deng, Y. H., Wang, S. J., Bai, X. Y., Luo, G. J., Wu, L. H., Chen, F., Wang, J. F., Li, Q., Li, C. J., Yang, Y. J., Hu, Z. Y. & Tian, S. Q. 2020 Spatiotemporal dynamics of soil moisture in the karst areas of China based on reanalysis and observations data. *Journal of Hydrology* **585**, 124744.

Ding, Y. L., Nie, Y. P., Chen, H. S., Wang, K. L. & Querejeta, J. I. 2020 Water uptake depth is coordinated with leaf water potential, water-use efficiency and drought vulnerability in karst vegetation. *New Phytologist Foundation* **229** (3), 1339–1353.

Duan, L. X., Huang, M. B. & Zhang, L. D. 2016 Differences in hydrological responses for different vegetation types on a steep slope on the Loess Plateau, China. *Journal of Hydrology* **537**, 356–366.

Eunhyung, L. & Sanghyun, K. 2019 Wavelet analysis of soil moisture measurements for hillslope hydrological processes. *Journal of Hydrology* **575**, 82–93.

Fu, T. G., Chen, H. G., Fu, Z. Y. & Wang, K. L. 2016 Surface soil water content and its controlling factors in a small karst catchment. *Environmental Earth Sciences* **75** (21), 1406.

Gao, J. B., Zuo, L. Y. & Liu, W. L. 2020 Environmental determinants impacting the spatial heterogeneity of karst ecosystem services in Southwest China. *Land Degradation and Development* **32** (4), 1718–1731.

Green, T. R. & Erskine, R. H. 2011 Measurement and inference of profile soil-water dynamics at different hillslope positions in a semiarid agricultural watershed. *Water Resources Research* **47** (12), 366–378.

Guo, X. X., Gong, X. P., Tang, Q. J., Chen, C. J., Jiang, G. H., Li, X. & Zou, Y. 2016 Research on the response process of soil moisture in typical karst hillside to rainfall. *China Karst* **35** (06), 629–638 (in Chinese).

Hou, G. R., Bi, H. X., Wei, X., Kong, L. X., Wang, N. & Zhou, Q. Z. 2018 Response of soil moisture to single-rainfall events under three vegetation types in the gully region of the Loess Plateau. *Sustainability* **10** (10), 1–17.

Huang, W. L. 1988 *Vegetation in Guizhou*. Guizhou People's Publishing House, Guiyang, Guizhou, China.

Laio, F., Porporato, A., Fernandez-Illescas, C. P. & Rodriguez-Iturbe, I. 2001 Plants in water-controlled ecosystems: active role in hydrologic processes and response to water stress: II. Probabilistic soil moisture dynamics. *Advances in Water Resources* **24** (7), 695–705.

Le, R. P. C., Aalto, J. & Luoto, M. 2013 Soil moisture's underestimated role in climate change impact modelling in low-energy systems. *Global Change Biology* **19** (10), 2965–2975.

Li, Q., Zhu, Q., Zheng, J. S., Liao, K. H. & Yang, G. S. 2015 Soil moisture response to rainfall in forestland and vegetable plot in Taihu Lake Basin, China. *Chinese Geographical Science* **25** (04), 426–437.

Li, X. Y., Li, Y., Chen, A. P., Gao, M. D., Slette, I. J. & Piao, S. L. 2019 The impact of the 2009/2010 drought on vegetation growth and terrestrial carbon balance in Southwest China. *Agricultural and Forest Meteorology* **269**, 239–248.

Li, Y., Liu, Z. & Liu, G. 2020 Dynamic variations in soil moisture in an epikarst fissure in the karst rocky desertification area. *Journal of Hydrology* **591** (7), 125587.

Li, Y. B., Yu, M., Zhang, H. & Xie, Y. X. 2022 From expansion to shrinkage – exploring the evolution and transition of karst rocky desertification in karst mountainous areas of Southwest China. *Land Degradation & Development*. doi:10.1002/ldr.4188.

Lin, H. & Zhou, X. 2008 Evidence of subsurface preferential flow using soil hydrologic monitoring in the Shale Hills catchment. *European Journal of Soil Science* **59** (1), 34–49.

Lozano-Parra, J., Schnabel, S. & Ceballos-Barbancho, A. 2015 The role of vegetation covers on soil wetting processes a rainfall event scale in scattered tree forestland of Mediterranean climate. *Journal of Hydrology* **529**, 951–961.

McColl, K. A., Alemohammad, S. H., Akbar, R., Konings, A. G., Yueh, S. & Entekhabi, D. 2017 The global distribution and dynamics of surface soil moisture. *Nature Geoscience* **10** (2), 100–104.

Peng, X. D., Dai, Q. H., Ding, G. J., Shi, D. M. & Li, C. J. 2020 Impact of vegetation restoration on soil properties in near-surface fissures located in karst rocky desertification regions. *Soil and Tillage Research* **200**, 104620.

Qiu, S. J., Peng, J., Zheng, H. N., Xu, Z. H., Meersmans, J. 2022 How can massive ecological restoration programs interplay with social-ecological systems? A review of research in the South China karst region. *Science of The Total Environment* **807**, 150723.

Sheng, M. Y., Xiong, K. G., Wang, L. G., Li, X. N., Li, R. & Tian, X. J. 2018 Response of soil physical and chemical properties to Rocky desertification succession in South China Karst. *Carbonates and Evaporites* **33** (1), 15–28.

Sun, F. X., Lü, Y. H., Wang, J. L., Hu, J. & Fu, B. J. 2015 Soil moisture dynamics of typical ecosystems in response to precipitation: a monitoring-based analysis of hydrological service in the Qilian Mountains. *Catena* **129** (1), 63–75.

Tian, J., Zhang, B. Q., He, C. S., Han, Z. B., Bogena, H. R. & Huisman, J. A. 2019 Dynamic response patterns of profile soil moisture wetting events under different land covers in the Mountainous area of the Heihe River Watershed, Northwest China. *Agricultural and Forest Meteorology* **271**, 225–239.

Wang, T. J., Zlotnik, V. A., Wedin, D. & Wally, K. D. 2008 Spatial trends in saturated hydraulic conductivity of vegetated dunes in the Nebraska Sand Hills: effects of depth and topography. *Journal of Hydrology* **349** (1–2), 88–97.

Wang, M., Ding, Z., Wu, C. Y., Song, L. S., Ma, M. G., Yu, P. J., Lu, B. Q. & Tang, X. G. 2020 Divergent responses of ecosystem water-use efficiency to extreme seasonal droughts in Southwest China. *Science of the Total Environmental* **760**, 143427.

Wiekenkamp, I., Huisman, J. A., Bogena, H. R., Lin, H. S. & Vereecken, H. 2016 Spatial and temporal occurrence of preferential flow in a forested headwater catchment. *Journal of Hydrology* **534**, 139–149.

Xiao, W. J., Yan, Y., Jiang, X. G., He, Z. L., Zou, X. G., You, X. H., Yang, Y. Y., Zeng, Z. Z. & Shi, W. Y. 2021 Different responses of ecohydrological processes in the re-vegetation area between the dip and anti-dip slope in a karst rocky desertification area in southwestern China. *Plant and Soil* **475** (1), 25–43.

Yang, J., Chen, H. S., Nie, Y. P. & Wang, K. L. 2019 Dynamic variations in profile soil water on karst hillslopes in Southwest China. *Catena* **172**, 655–663.

Yang, Z. C., Ke, Q. H., Ma, Q. H., Cao, Z. H. & Zhang, K. L. 2021 Response of soil moisture on yellow soil slope in karst area to rainfall. *Journal of Soil and Water Conservation* **35** (02), 75–79 (in Chinese).

Yolanda, C., Rodríguez-Caballero, E., Contreras, S., Villagarcia, L., Li, X. Y., Solé-Benet, A. & Domingo, F. 2016 Vertical and lateral soil moisture patterns on a Mediterranean karst hillslope. *Journal of Hydrology and Hydromechanics* **64** (3), 209–217.

Zhang, J. G., Chen, H. S., Su, Y. R., Shi, Y., Zhang, W. & Kong, X. L. 2011 Spatial variability of surface soil moisture in a depression area of karst region. *Clean-Soil, Air, Water* **39** (7), 619–625.

Zhang, L., Xiao, J. F., Li, J., Wang, K., Lei, L. P. & Guo, H. D. 2012 The 2010 spring drought reduced primary productivity in southwestern China. *Environmental Research Letters* **7**, 045706.

Zhao, Y. L., Wang, Y. Q., Wang, L., Zhang, X. Y., Yu, Y. L., Zhao, J., Lin, H., Chen, Y. P., Zhou, W. J. & An, Z. S. 2019 Exploring the role of land restoration in the spatial patterns of deep soil water at watershed scales. *Catena* **172**, 387–396.

Zhao, Z. M., Shen, Y. X., Wang, Q. G. & Jiang, R. H. 2020 The temporal stability of soil moisture spatial pattern and its influencing factors in rocky environments. *Catena* **187**, 104418.

Zhou, Q. W., Sun, Z. R., Liu, X. L., Wei, X. C., Peng, Z., Yue, C. W. & Luo, Y. X. 2019 Temporal soil moisture variations in different vegetation cover types in karst areas of southwest China: a plot scale case study. *Water* **11** (7), 1423.

First received 9 March 2022; accepted in revised form 13 September 2022. Available online 29 September 2022